

Analysis of pinning in $\text{NdBa}_2\text{Cu}_3\text{O}_{7-\delta}$ superconductors

M. R. Koblishka,* A. J. J. van Dalen,† T. Higuchi, S. I. Yoo, and M. Murakami

Superconductivity Research Laboratory, International Superconductivity Technology Center, 1-16-25, Shibaura, Minato-ku, Tokyo 105, Japan

(Received 3 December 1997)

Current densities j_s and volume pinning forces F_p are obtained in a wide temperature ($5 \leq T \leq 92$ K) and field range ($0 \leq \mu_0 H_a \leq 9$ T) on different $\text{NdBa}_2\text{Cu}_3\text{O}_{7-\delta}$ samples. Above 60 K a good scaling of the volume pinning force F_p versus the reduced field $h = H_a/H_{\text{irr}}$ can be established. The scaled pinning curves are compared to several theoretical predictions. Experimental evidence for strong pinning at extended superconducting defects (interaction volume $V_{\text{pin}} \sim \xi^2 d$) is given. These defects are ascribed to spatial composition fluctuations found in light rare-earth superconductors, providing a scatter of the transition temperature T_c . Such a pinning mechanism is especially important for applications of high- T_c superconductors operating at $T = 77$ K. [S0163-1829(98)05129-7]

I. INTRODUCTION

Flux pinning is one of the crucial problems in the development of technical high- T_c superconductors, especially because of the high operation temperature (77 K) aimed for in applications. The pinning properties are in general strongly dependent on temperature. At elevated temperatures, cross-overs between pinning regimes, melting of the vortex lattice, etc., may occur, thus diminishing the current capacity of the superconductor.^{1,2} To prepare a high- T_c superconductor suitable for applications, melt processing has proven to be an important step forward.³ More recently, the development of the light rare-earth superconductors of 123 type containing Nd, Sm, Eu, Gd, instead of Y presented a novel approach to the problem. These superconductors are characterized by an enhanced transition temperature T_c ranging between 92 and 96 K and the presence of composition fluctuations throughout the sample as the light rare-earth atoms may substitute on the Ba sites.⁴ These composition fluctuations are technologically interesting as they may give rise to additional flux pinning⁵ by a scatter of T_c or κ (δT_c pinning^{1,6} or $\Delta\kappa$ pinning⁷⁻¹⁰). $\text{NdBa}_2\text{Cu}_3\text{O}_{7-\delta}$ (NdBCO) samples show a very pronounced fishtail maximum at relatively high fields as compared to ordinary $\text{YBa}_2\text{Cu}_3\text{O}_{7-\delta}$ (YBCO) samples.¹¹⁻¹³ Especially the properties at elevated temperatures around 77 K are considerably improved as compared to YBCO, thus making NdBCO an interesting candidate for future applications.

A very fruitful tool to investigate the pinning properties in superconductors is the determination of the volume pinning forces $F_p = j_c \times B$ from the critical current densities j_c . In conventional superconductors, a scaling of F_p was obtained when plotting the normalized pinning force $F_p/F_{p,\text{max}}$ versus the reduced field $h = H_a/H_{c2}$, where H_{c2} denotes the upper critical field. This scaling implies $F_p = [H_{c2}(T)]^m \times f(h)^n$ with m and n being numerical parameters describing the actual pinning mechanism;⁷ $f(h)$ depends only on the reduced magnetic field h .^{8,9} In literature, several pinning functions $f(h)$ are described depending on the size and character of the defects providing the pinning based on the study of conven-

tional, hard type-II superconductors.⁷⁻¹⁰ For various high- T_c materials, the scaling of F_p is found as well,¹⁴⁻¹⁶ however, experiments have shown that the appropriate scaling field is the irreversibility field H_{irr} instead of H_{c2} .^{17,18} In general, any determination of the parameters m and n from scaling laws is more significant than that obtained only from measurements of the irreversibility line.¹⁸

In this paper, we present an analysis of the scaled volume pinning forces in NdBCO samples (both a single crystal and a melt-processed sample) based on the description by Dew-Hughes⁹ in the temperature range from 60 to 92 K in order to prove the pinning by composition fluctuations. This paper is organized as follows. In Sec. II, the sample preparation and some experimental details are outlined. Section III presents the plots of the volume pinning forces for both samples. Several approaches to analyze the data are discussed. Finally, in Sec. IV, some conclusions are drawn.

II. EXPERIMENTAL PROCEDURE

Single crystals of NdBCO were grown by a flux growth method in controlled oxygen atmosphere as described in Ref. 19. The selected crystal was densely twinned, and had the shape of a thin platelet with dimensions $0.79 \times 0.63 \times 0.08$ mm³ with the c axis perpendicular to the sample surface. The sample showed a sharp transition to the superconducting state with a $T_{c,\text{onset}}$ of 93.8 K. The melt processed sample was prepared via the oxygen-controlled melt growth process (OCMG) described in Ref. 4. Additionally, the sample contained fine $\text{Nd}_4\text{Ba}_2\text{Cu}_2\text{O}_{10}$ (Nd-422) inclusions with an average size of 1.7 μm . Finally, this sample was cut into a cubic shape with dimensions $1.92 \times 1.86 \times 0.3$ mm³.

Magnetization loops were measured in the temperature range $5 \leq T \leq 92$ K using a Quantum Design MPMS-7 superconducting quantum interference device (SQUID) magnetometer equipped with a 7 T superconducting magnet. In order to avoid field inhomogeneities, the scan length was set to 15 mm. Some additional measurements were performed using a PAR 155 vibrating sample magnetometer (VSM) mounted in a JANIS cryostat with a maximum field of ± 9 T. The magnetic field is applied parallel to the c axis of the sample. The

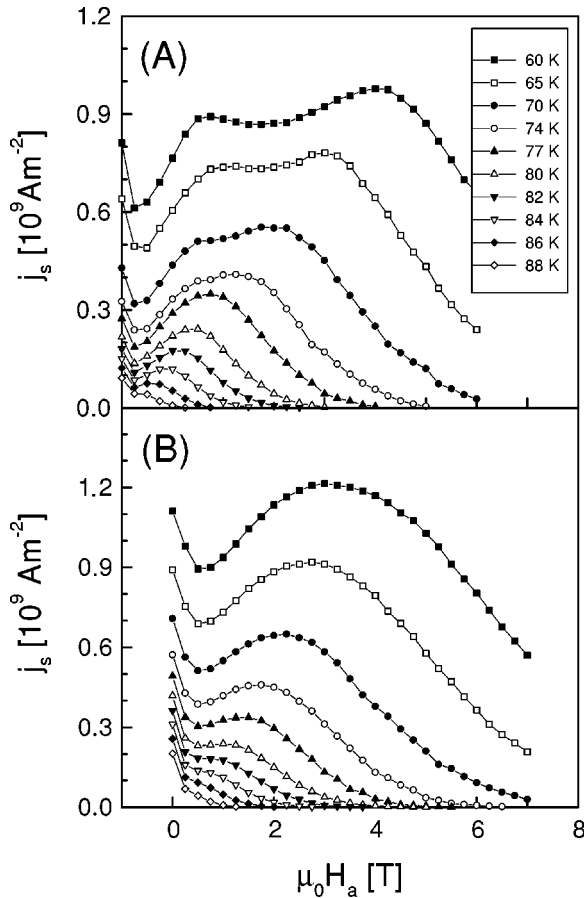


FIG. 1. Field dependence of the critical current density j_s of the single crystal (a) and the melt-processed $\text{NdBa}_2\text{Cu}_3\text{O}_{7-\delta}$ sample (b), obtained from magnetic hysteresis loops measured at various T . Note in (a) the presence of an additional peak at ≈ 2 T, which is independent of temperature. At 77 K, both peaks merge together.

induced current densities $j_s(T, H_a)$ were calculated using the extended Bean model.

III. RESULTS AND DISCUSSION

In Fig. 1, the field dependence of the induced current density j_s in both samples is shown for temperatures between 60 and 88 K. Both samples show a very pronounced fishtail effect, with the maxima at quite large fields as compared to YBCO. In addition, in the single crystal we observe a second peak at $\mu_0 H_a \approx 2$ T, being independent of temperature. At 77 K, the two peaks merge together and form one broad peak. The occurrence of this extra peak, which is not present in the OCMG sample, is discussed in more detail elsewhere.¹¹ A comparison of the two samples shows that the measured current densities j_s are slightly larger for the OCMG sample.

Figure 2 presents the temperature dependence of the irreversibility field H_{irr} and of the position of the fishtail peak H_p for both samples. The data for H_{irr} are obtained from the magnetization loops measured either by SQUID or VSM, defined as the onset of irreversibility. The values of H_{irr} for $T < 70$ K are obtained by means of the scaling as shown below in Fig. 3. The location of the irreversibility line is found to be quite similar for both samples, but there is a tendency

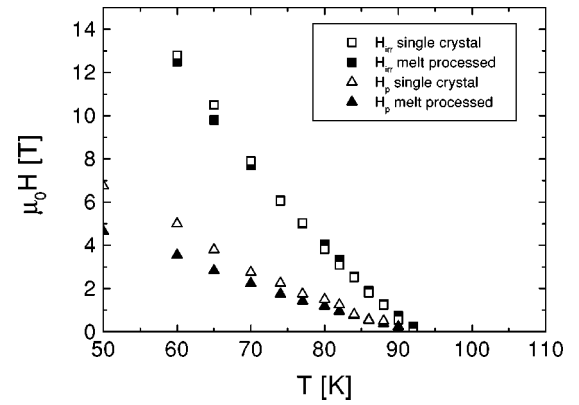


FIG. 2. Temperature dependence of the irreversibility field H_{irr} and of the peak position of the fishtail peak H_p for both samples.

of the single crystal data towards larger H_{irr} below 70 K reflecting the influence of the more pronounced fishtail peak H_p of the single crystal. From 80 K up to T_c , the values of H_{irr} of the OCMG sample are slightly larger.

In Fig. 3, the plots of the normalized volume pinning force $F_p/F_{p,\text{max}}$ versus the reduced field $h = H_a/H_{\text{irr}}$, are shown for both samples. To determine h , only the experimentally obtained data were used; the corrections necessary were always within the experimental error. For $T < 70$ K, h was treated as a free parameter, but following the temperature dependence $(1 - T/T^*)^p$ with $T^* = T_c$ and $p \approx 1.2$.^{11,20} In both cases, a very good scaling can be obtained. The po-

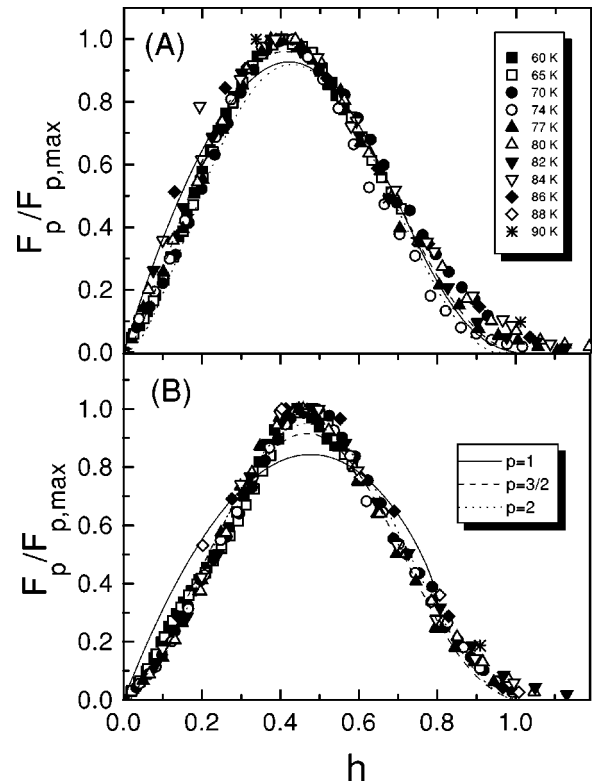


FIG. 3. Plots of the scaled volume pinning forces $F_p/F_{p,\text{max}}$ versus the reduced field $h = H_a/H_{\text{irr}}$ for the single crystal (a) and the melt-processed sample (b) in the temperature range $60 \text{ K} \geq T \geq 90 \text{ K}$. The lines are the results of Eq. (2) with $q = 1$ and different p .

sition of the peak h_0 is determined to be 0.48 (single crystal) and 0.42 (OCMG). The data were then fitted to the functional dependence given by

$$F_p/F_{p,\max} = A(h)^p(1-h)^q, \quad (1)$$

with A = numerical parameter, p and q are describing the actual pinning mechanism. The position of the maximum in the F_p plot h_0 is given by $p/p+q$. Best fits to our data yield $A = 20.31 \pm 3$, $p = 2.08 \pm 0.09$, $q = 2.35 \pm 0.11$ (single crystal) and $A = 11.7 \pm 1.7$, $p = 1.48 \pm 0.08$, $b = 2.23 \pm 0.12$ (melt-processed sample). The data of YBCO in the literature typically yield $p=2$ and $q=4$, implying a peak at $h_0=0.33$.^{14,21,22} For melt-processed YBCO with fine Y₂BaCuO₅ (Y-211) inclusions similar values are found.²³

It is important to point out that the intermediate peak in the $j_s(H_a)$ data of the single crystal form a small shoulder at $h \approx 0.18$. This indicates indeed an anomalous enhancement of the pinning force, which is presumably due to a matching of the flux line lattice to the twin structure.¹¹

It is in general not trivial to analyze the F_p plots for the actually acting pinning mechanism. To describe the pinning in high- T_c materials, we can safely assume that core pinning is dominant due to the large κ values. This leaves two different sources of pinning; either by nonsuperconducting (normal) particles embedded in the superconducting matrix leading to a scatter of the electron mean free path (δl pinning) or pinning provided by spatial variations of the Ginzburg parameter associated with fluctuations in the transition temperature T_c [δT_c ($\Delta\kappa$) pinning].^{1,6} Pinning is different for various sizes of pinning sites compared to the inter flux line spacing $d = 2/\sqrt{3}(\Phi_0/B)^{0.5}$, where Φ_0 denotes the flux quantum. The interaction volume V_{pin} of point pins is $\sim \xi^3$, whereas volume pins $V_{\text{pin}} \sim d^3$. High- T_c superconductors contain several different sources of pinning which may operate simultaneously. Based on experiments controlling the oxygen content in single crystals of YBCO prepared in BaZrO₃ crucibles,²⁴ we conclude that oxygen vacancies (clusters) in conjunction with metal impurities are the main pinning source in YBCO, causing the so-called fishtail shape of magnetization loops.²⁵

Furthermore, the effects of flux creep play an important role, especially at elevated temperatures. In general, the pinning analysis is only valid for the *true* critical current densities j_c which is by definition not affected by flux creep, so $j_c \leq j_s$.⁶ For high h (i.e., close to the irreversibility line), creep effects are most important and so the deviations from j_c will be large. For example, the F_p plots of Bi-based superconductors show typically a peak at $h_0 \approx 0.25$, followed by a long rounded off tail towards high h . Several authors^{17,18,26} discussed their F_p plots of Bi-based superconductors within the framework of collective pinning theory.¹ This approach enables one to explain why the scaling field for high- T_c superconductors is H_{irr} instead of H_{c2} .²⁷

Elastic pinning theory⁸ predicts that the peak in $F_p(h)$ occurs when pinning gives way to shear. This process is assumed to be independent of the pinning strength, which, as it increases, causes the peak to move to lower fields. This approach yields best results for high- T_c superconductors

with a dense distribution of weak pins. Such a situation may be realized, e.g., in twin-free YBCO single crystals.

A fit to our data using the elastic theory and using the descriptions given in Refs. 17,18,26 fails, mainly due to the peak position at $h_0 \approx 0.5$, which cannot be reproduced by reasonable fit parameters. Due to the assumptions made, these approaches are adapted to the low peak position^{17,18,26,28} at $h_0 \approx 0.2$ and the large creep effects found in Bi-based high- T_c materials.

In contrast to this, the model of Dew-Hughes⁹ is a direct summation model of the elementary pinning forces. This approach ignores flux line elasticity, and does not contain effects of flux creep. However, this model may predict many forms of pinning functions and can describe various pinning types. Therefore, it is ideally suited for the analysis of F_p data for an unknown pinning mechanism.

All this leads us to employ the model of Dew-Hughes for the following reasons. (i) Our data gave a natural scaling, which we want to analyze for the underlying pinning mechanism. (ii) The relaxation in NdBCO does not play such an important role as in many other high- T_c systems; in the peak region flux creep is even considerably suppressed.¹² Furthermore, flux creep effects can be incorporated in the model. (iii) There may be many different pinning mechanisms active simultaneously in high- T_c superconductors. It is the important task to find the dominating one; this dominating pinning mechanism will in turn be responsible for the location of the peak in $F_p(h)$. The pinning functions may even be combined, which can be important if, e.g., a superconducting pinning site is rendered normal in large applied fields. (iv) The composition fluctuations in NdBCO are strong pinning sites (fishtail position at large fields), which cannot be described by elastic pinning theory.

In this model, there are six different pinning functions $f(h)$ describing the core pinning using Eq. (1). (1) $p=0$, $q=2$: normal, volume pinning; (2) $p=1$, $q=1$: $\Delta\kappa$ -pinning, volume pins; (3) $p=1/2$, $q=2$: normal, surface pins; (4) $p=3/2$, $q=1$: $\Delta\kappa$ -pinning, surface pins; (5) $p=1$, $q=2$: normal, point pins; and (6) $p=2$, $q=1$: $\Delta\kappa$ -pinning, point pins. Additionally, (3) is predicted by Kramer⁸ for shear-breaking in the case of a set of planar pins.

To account for flux creep effects in the model of Dew-Hughes, we replace j_c by an expression based on collective pinning theory.²⁹ This yields

$$\frac{F_p}{F_{p,\max}} = A(h)^p(1-h)^q(1 + \mu CkTh^{-n}/U_c)^{-1/\mu}, \quad (2)$$

with U_c denoting the pinning potential, C is defined by $U[j_s(T), H_a] = kTC$, and k is the Boltzmann constant. This expression is used to fit the curves shown in Fig. 3; in the fit, the value for q is set equal to 1 (following functions 2, 4, and 6), and the whole creep term is used as one fit parameter. These fits are shown in Fig. 3(a) and 3(b). This confirms that the high peak position found in the NdBCO samples is indeed a fingerprint of δT_c ($\Delta\kappa$) pinning.

In Fig. 4, we present a plot of all six pinning functions together with the best fits to the experimental data. The composition fluctuations in NdBCO are about 10 nm in size,^{30,31}

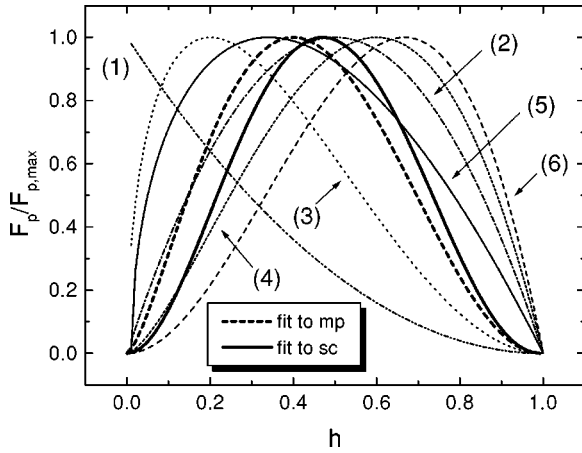


FIG. 4. Pinning functions $f(h)$ following the description of Dew-Hughes (Ref. 9) compared to the best fits to our experimental data of both samples (sc: single crystal, mp: OCMG melt-processed sample). For details of the pinning functions, see text. The fits are best described by functions (2) and (4). Note that the pinning of the OCMG sample is larger than in the single crystal for small h .

thus making them most effective at high fields. Following the classification given above, we are dealing with surface or volume pins causing variations of the superconducting properties. This implies that the pinning functions (2) and (4) should be followed by our data. However, mixtures of pinning mechanisms are possible plus that all other well-known pinning sources are also present. From the data, however, we can deduce that the pinning described by functions (2), (4) is dominant, thus being responsible for the peak position. At low h , the single crystal data tend to follow function (4), but with increasing h function (2) is approached. The data of the melt-processed sample are close to function (2) up to the peak region. At large h , the influence of creep manifests itself in a suppression of the measured j_s , but it is also very likely that some areas of lower T_c are rendered normal by the field, so that now pinning at normal inclusions is provided. This would imply that functions (1) or (3) may contribute to the pinning, thus reducing the effectivity of the dominant pinning described by functions (2) or (4). All other pinning mechanisms only give minor contributions. The pinning at point defects yields always a wrong description of our data.

It is important to note that in the F_p plots only one large maximum is found, and the entire $F_p(h)$ behavior can be described using one single pinning function. This is in stark contrast to conventional superconductors showing the peak effect as in this case the shape of the F_p curve is modified by a narrow but large additional peak at high h . If the pinning is field induced, the pinning should be weak for low h and have a peak following function (2) or (4) with increasing h . The onset of field-induced pinning should be clearly visible in the F_p plots, i.e., it is then not possible to describe the pinning by Eqs. (1) or (2) alone. Such a situation is also found for a high- T_c superconductor; in Ref. 32 the pinning of an $\text{YBa}_2\text{Cu}_4\text{O}_8$ single crystal could only be described by two pinning functions of the same type as Eq. (1).

The OCMG sample contains finely dispersed inclusions of $\text{Nd}_4\text{Ba}_2\text{Cu}_2\text{O}_{10}$ (Nd-422) phase, which can act as pinning sites in analogy to the Y-211 inclusions in melt-processed

YBCO. If this attempt is successful, we may expect a combination of the pinning functions (3) and (2) describing the pinning in the entire temperature range. Indeed, we see from Fig. 4, that F_p is raising much faster with increasing h in the melt-processed sample. The ideal situation would be the formation of a broad peak covering a large area from $h \approx 0.2$ to 0.6. However, further work is required to optimize the Nd-422 particle size in order to achieve optimal pinning properties.

In Ref. 6 strong evidence for δl pinning was presented for YBCO thin films. In contrast to this, several authors found evidence for δT_c pinning in Pr-doped YBCO and (K,Ba)BiO₃ single crystals.³³ As the composition fluctuations in NdBCO provide variations in T_c , but with the advantage that the overall T_c is not reduced as in the case of Pr doping, this pinning is most effective just at elevated temperatures. The δT_c pinning is characterized by its temperature dependence of the pinning potential, which is increasing with increasing T up to $T/T_c < 0.7$.^{1,6} Indeed, the measured pinning potentials of NdBCO (Ref. 12) show such a behavior.

These observations lead straightforwardly to the conclusion that the ideal pinning center for high- T_c materials at ≈ 77 K is a superconducting one with at least a size of the order of $\xi^2 d$ providing a scatter in T_c . The composition fluctuations in NdBCO are optimally suited as the scatter in T_c is provided avoiding the strong depression of j_s by, e.g., Pr doping.³³ As shown in Ref. 34, the physics of flux pinning in NdBCO is strongly related to that of the Pr-doped YBCO. Such a pinning mechanism would especially be important for the Bi- and Tl-based high- T_c materials ($\text{Bi}_2\text{Sr}_2\text{CaCu}_2\text{O}_{8+\delta}$ and $\text{Bi}_2\text{Sr}_2\text{Ca}_2\text{Cu}_3\text{O}_{10+\delta}$), where strong bulk pinning vanishes above 60 K and is then mainly governed by geometrical barriers.³⁵ Normal conducting pinning sites will always cause the peak in F_p at low h . However, the additional presence of strong nonsuperconducting pinning sites within the samples should lead to broad peaks in the F_p diagrams, so the overall $j_s(T, H_a)$ could be improved considerably.

IV. CONCLUSIONS

As a conclusion, we may state that the peak positions in the F_p diagram close to 0.5 are a strong indication that indeed pinning at composition fluctuations providing a scatter of T_c is active in NdBCO. This additional pinning mechanism is responsible for the position of the fishtail peak at high h and for the large current densities at around 77 K. Furthermore, the ideal pinning for high- T_c materials operating at 77 K would be a combination of a superconducting one ($V_{\text{pin}} \geq \xi^2 d$) providing a scatter in T_c and of strong pinning at normal inclusions being active mainly at low temperatures.

ACKNOWLEDGMENTS

This work was partially supported by the New Energy and Industrial Technology Development Organization (NEDO) for the R & D of the Industrial Science and Technology Frontier Program. We thank K. Sawada and H. Kojo for the preparation of the samples. M.K. and A.D. are grateful for support from Japanese Science and Technology Agency (STA).

- *Present address: Department of Physics, Norwegian University of Science and Technology, N-7034 Trondheim, Norway.
- †Present address: Materials Science Division, Argonne National Laboratory, Argonne, Illinois 60439.
- ¹G. Blatter, M. V. Feigel'man, V. B. Geshkenbein, A. I. Larkin, and V. M. Vinokur, *Rev. Mod. Phys.* **66**, 1125 (1994); M. V. Feigel'man, V. B. Geshkenbein, and V. M. Vinokur, *Phys. Rev. B* **43**, 6263 (1991).
- ²D. Majer, E. Zeldov, and M. Konczykowski, *Phys. Rev. Lett.* **75**, 1166 (1995); B. Khaykovich, E. Zeldov, D. Majer, T. W. Li, P. H. Kes, and M. Konczykowski, *ibid.* **76**, 2555 (1996); U. Welp, J. A. Fendrich, W. K. Kwok, G. W. Crabtree, and B. W. Veal, *ibid.* **76**, 4809 (1996).
- ³S. Jin, T. H. Tiefel, R. C. Sherwood, R. B. van Dover, M. E. Davis, G. W. Kammlott, and R. A. Fastnacht, *Phys. Rev. B* **37**, 7850 (1988); M. Murakami, M. Morita, and N. Koyama, *Jpn. J. Appl. Phys., Part 2* **28**, L1125 (1989).
- ⁴For a recent review, see, M. Murakami, N. Sakai, T. Higuchi, and S. I. Yoo, *Supercond. Sci. Technol.* **9**, 1015 (1996).
- ⁵M. Murakami, S. I. Yoo, T. Higuchi, N. Sakai, J. Weltz, N. Koshizuka, and S. Tanaka, *Jpn. J. Appl. Phys., Part 2* **33**, L715 (1994); S. I. Yoo, N. Sakai, H. Takaichi, T. Higuchi, and M. Murakami, *Appl. Phys. Lett.* **65**, 633 (1994); M. Murakami, S. I. Yoo, T. Higuchi, N. Sakai, M. Watahiki, N. Koshizuka, and S. Tanaka, *Physica C* **235-240**, 2781 (1994).
- ⁶R. Griessen, H. H. Wen, A. J. J. van Dalen, B. Dam, J. Rector, H. G. Schnack, S. Libbrecht, E. Osquiguil, and Y. Bruynseraede, *Phys. Rev. Lett.* **72**, 1910 (1994).
- ⁷W. A. Fietz and W. W. Webb, *Phys. Rev.* **178**, 657 (1969).
- ⁸E. J. Kramer, *J. Appl. Phys.* **44**, 1360 (1973).
- ⁹D. Dew-Hughes, *Philos. Mag.* **30**, 293 (1974).
- ¹⁰H. Ullmaier, *Irreversible Properties Of Type II Superconductors* (Springer-Verlag, Berlin, 1975), Chap. 3; A. M. Campbell and J. E. Evetts, *Adv. Phys.* **21**, 199 (1972).
- ¹¹M. R. Koblischka, A. J. J. van Dalen, T. Higuchi, K. Sawada, S. I. Yoo, and M. Murakami, *Phys. Rev. B* **54**, R6893 (1996).
- ¹²A. J. J. van Dalen, M. R. Koblischka, K. Sawada, H. Kojo, T. Higuchi, and M. Murakami, *Supercond. Sci. Technol.* **9**, 659 (1996).
- ¹³T. Egi, J. G. Wen, K. Kuroda, H. Mori, H. Unoki, and N. Koshizuka, *Physica C* **270**, 223 (1996).
- ¹⁴L. Civale, M. W. McElfresh, A. D. Marwick, F. Holtzberg, C. Feild, J. R. Thompson, and D. K. Christen, *Phys. Rev. B* **43**, 13 732 (1991); L. Klein, E. R. Yacoby, Y. Yeshurun, A. Erb, G. Müller-Vogt, V. Breit, and H. Wühl, *ibid.* **49**, 4403 (1994); J. S. Satchell, R. G. Humphreys, N. G. Chow, J. A. Edwards, and M. J. Kane, *Nature (London)* **334**, 331 (1988); T. Nishizaki, T. Aomine, I. Fujii, K. Yamamoto, S. Yoshii, T. Terashima, and Y. Bando, *Physica C* **181**, 223 (1991).
- ¹⁵K. Kishio, Y. Nakayama, N. Motohira, T. Noda, T. Kobayashi, K. Kitazawa, K. Yamafuji, I. Tanaka, and H. Kojima, *Supercond. Sci. Technol.* **5**, S69 (1992).
- ¹⁶M. R. Koblischka, *Physica C* **282-287**, 2197 (1997).
- ¹⁷H. Yamasaki, K. Endo, S. Kosaka, M. Umeda, S. Yoshida, and K. Kajimura, *Phys. Rev. Lett.* **70**, 3331 (1993).
- ¹⁸P. Fabbriatore, C. Priano, A. Sciutti, G. Gemme, R. Musenich, R. Parodi, F. Gömöry, and J. R. Thompson, *Phys. Rev. B* **54**, 12 543 (1996).
- ¹⁹K. Sawada, S. I. Yoo, N. Sakai, T. Higuchi, and M. Murakami, *4th Euro Ceramics*, edited by A. Barone, D. Fiorani, and A. Tampieri (Gruppo Editoriale Faenza Editrice, Faenza, 1995), Vol. 6, p. 293.
- ²⁰M. R. Koblischka, A. J. J. van Dalen, T. Higuchi, K. Sawada, H. Kojo, S. I. Yoo, and M. Murakami, in *3rd EUCAS Conference*, Veldhoven, The Netherlands, IOP Conf. Proc. No. 158 (Institute of Physics and Physical Society, London, 1997), p. 1145.
- ²¹J. N. Li, F. R. de Boer, L. W. Roeland, M. J. V. Menken, K. Kadowaki, A. A. Menovsky, J. J. M. Franse, and P. H. Kes, *Physica C* **169**, 81 (1990).
- ²²J. Y. Juang, S. J. Wang, T. M. Uen, Y. S. Gou, H. L. Chang, and C. Wang, *Phys. Rev. B* **46**, 1188 (1992).
- ²³M. Murakami, in *Melt Processed High Temperature Superconductors*, edited by M. Murakami (World Scientific, Singapore, 1992).
- ²⁴A. Erb, J.-Y. Genoud, F. Marti, M. Däumling, E. Walker, and R. Flükiger, *J. Low Temp. Phys.* **105**, 1023 (1996).
- ²⁵See, e.g., M. Jirsa, L. Püst, D. Dlouhy, and M. R. Koblischka, *Phys. Rev. B* **55**, 3276 (1997).
- ²⁶S. L. Prischepa, C. Attanasio, C. Coccorese, L. Maritato, F. Poutrier, M. Salvato, and V. N. Kushnir, *J. Appl. Phys.* **79**, 4228 (1996).
- ²⁷J. D. Hettinger, A. G. Swanson, W. J. Skocpol, J. S. Brooks, J. M. Graybeal, P. M. Mankiewich, R. E. Howard, B. L. Straughn, and E. G. Burkhardt, *Phys. Rev. Lett.* **62**, 2044 (1989).
- ²⁸J. Löhle, K. Mattenberger, O. Vogt, and P. Wachter, *J. Appl. Phys.* **76**, 7446 (1994).
- ²⁹J. R. Thompson, Y. R. Sun, L. Civale, A. P. Malozemoff, M. W. McElfresh, A. D. Marwick, and F. Holtzberg, *Phys. Rev. B* **47**, 14 440 (1993).
- ³⁰T. Egi, J. G. Wen, K. Kuroda, H. Unoki, and N. Koshizuka, *Appl. Phys. Lett.* **67**, 2406 (1995).
- ³¹Using scanning tunneling microscopy on NdBCO samples, several regions of different color were found on the sample surface with a dimension of about 10 nm. These defects are ascribed to the composition fluctuations. For details, see Ref. 30.
- ³²A. Wisniewski, R. Puzniak, M. Baran, R. Szymczak, J. Karpinski, and H. Schwer, in *Critical Currents in Superconductors*, Proceedings of the 8th IWCC, Kitakyushu, Japan, 1996 (World Scientific, Singapore, 1996), p. 381.
- ³³H. H. Wen, Z. X. Zhao, Y. G. Xiao, B. Yin, and J. W. Li, *Physica C* **251**, 371 (1995); W. Harneit, T. Klein, L. Baril, and C. Escribe-Filippini, *Europhys. Lett.* **36**, 141 (1996).
- ³⁴H. A. Blackstead and J. D. Dow, *Appl. Phys. Lett.* **70**, 1891 (1997).
- ³⁵E. Zeldov, D. Majer, M. Konczykowski, A. I. Larkin, V. M. Vinokur, V. B. Geshkenbein, N. Chikumoto, and H. Shtrikman, *Europhys. Lett.* **30**, 367 (1995); E. Zeldov, A. I. Larkin, V. B. Geshkenbein, M. Konczykowski, D. Majer, B. Khaykovich, V. M. Vinokur, and H. Shtrikman, *Phys. Rev. Lett.* **73**, 1428 (1994).